

Adaptive Boosting for Domain Adaptation: Towards Robust Predictions in Scene Segmentation

Zhedong Zheng and Yi Yang, *Senior Member, IEEE*

Abstract—Domain adaptation is to transfer the shared knowledge learned from the source domain to a new environment, *i.e.*, target domain. One common practice is to train the model on both labeled source-domain data and unlabeled target-domain data. Yet the learned models are usually biased due to the strong supervision of the source domain. Most researchers adopt the early-stopping strategy to prevent over-fitting, but when to stop training remains a challenging problem since the lack of the target-domain validation set. In this paper, we propose one efficient bootstrapping method, called Adaboost Student, explicitly learning complementary models during training and liberating users from empirical early stopping. Adaboost Student combines the deep model learning with the conventional training strategy, *i.e.*, adaptive boosting, and enables interactions between learned models and the data sampler. We adopt one adaptive data sampler to progressively facilitate learning on hard samples and aggregate “weak” models to prevent over-fitting. Extensive experiments show that (1) Without the need to worry about the stopping time, AdaBoost Student provides one robust solution by efficient complementary model learning during training. (2) AdaBoost Student is orthogonal to most domain adaptation methods, which can be combined with existing approaches to further improve the state-of-the-art performance. We have achieved competitive results on three widely-used scene segmentation domain adaptation benchmarks.

Index Terms—Domain Adaptation, Scene Segmentation.

I. INTRODUCTION

IN recent years, deep learning approaches have achieved significant improvement in many computer vision fields, including semantic segmentation [1], [2]. However, improving the scalability of deeply-learned models remains a challenging task. For instance, the segmentation models learned on the data collected on sunny days usually perform terribly in different environments, such as rainy days and foggy days [3]. One straightforward idea is to collect more training data for the target environment and re-train one domain-specific model for inference. However, it is usually unaffordable to annotate large-scale datasets for every target scenario, especially for the tasks demanding pixel-wise annotations, *e.g.*, scene segmentation. Therefore, researchers resort to domain adaptation techniques [4] to “borrow” the common knowledge from homogeneous datasets, *e.g.*, labeled source-domain data. The source-domain data can be the synthetic data generated by game engines, such as GTA5 [5], or the large-scale data collected in other real-world scenarios [6]. In this way, we can largely save the annotation cost as well as the training time to achieve competitive results in the target domain.

Zhedong Zheng and Yi Yang are with Centre for Artificial Intelligence, University of Technology Sydney, NSW, Australia. E-mail: zdzheng12@gmail.com, yi.yang@uts.edu.au

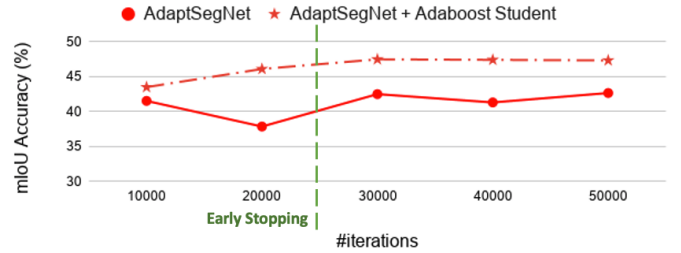


Fig. 1. The sensitivity analysis of model on the GTA5 [5] → Cityscapes [6] benchmark in the first 50000 iterations on the target-domain test set. We re-implement the widely-used method AdaptSegNet [13], and observe the prediction fluctuation at different training iterations. The proposed Adaboost Student makes the model free from the early-stopping trick and can efficiently converge to one competitive performance on the target domain. For instance, the empirical early-stopping time is usually set at the 25,000-th iteration [17], which is sub-optimal.

The common practice is to train the segmentation model on both labeled source-domain data and unlabeled target-domain data. Most existing works focus on the domain alignment, minimizing the gap between the source domain and the target domain [7], [8], [9]. Several early attempts leverage generative models to transfer the image style in the pixel level [10], [11], while other works concentrate on narrowing the semantic gap in the feature space [12]. For example, Tsai *et al.* [13], [14] and Luo *et al.* [15], [16] harness the adversarial loss to encourage the segmentation model to learn domain-invariant features.

However, one inherent problem exists in the scene segmentation domain adaptation. Due to the strong supervision on the source-domain label, we observe that the model is still prone to over-fitting the source domain, leading to the unstable prediction on the target domain (see Figure 1). Although several researchers adopt the early-stopping strategy to prevent over-fitting [15], [16], [17], when to stop the training remains challenging. The unstable prediction not only compromises the method re-implementation, but also harms users to select the final model in the real-world application.

In an attempt to overcome the above-mentioned challenge, this paper adopts the spirit of one conventional training strategy, *i.e.*, adaptive boosting [18], with the deeply-learned model to facilitate learning complementary models and progressively improve the model scalability. In particular, we gradually provide more sampling probability to the “hard” samples that achieve high prediction variance in the current model. In this way, we can efficiently obtain several complementary models during one-time training rather than training multiple independent models as the conventional adaptive

boosting [18]. Aggregating such model snapshots provide more robust predictions on unlabeled target domain data and, more importantly, prevents the model from over-fitting. As a result, we observe a consistent improvement over other domain adaptation approaches on three prevailing benchmarks.

To summarize, our contributions are:

- an efficient bootstrapping method for scene segmentation domain adaptation, AdaBoost Student, which enables interactions between learned models and the data sampler, and aggregates the “weak” model snapshots to prevent over-fitting. AdaBoost Student makes users free from the empirical early stopping trick; and
- an adaptive data sampler to progressively increase the sampling probability of hard samples with ambiguous predictions, facilitating the complementary model learning. The criterion of hard sample selection is based on the prediction variance in the unlabeled target-domain data; and
- a demonstration that the proposed approach has a consistent improvement over existing methods on two synthetic-to-real benchmarks and one cross-city benchmark.

II. RELATED WORK

A. Semantic Segmentation Adaptation

There are two big families of segmentation adaptation. One line of works [13], [14], [15], [19], [20], [21], [8] concentrates on the domain alignment. Some pioneering works [10], [11] leverage the CycleGAN [22] to transfer the image style to the target domain, minimizing the biases from the source domain. Taking one step further, Wu *et al.* [3] and Yue *et al.* [23] transfer the input images into different styles, such as rainy and foggy, to learn domain-invariant features. In contrast, several works do not change the image style in the pixel level, but leverage the adversarial loss to disentangle the shared knowledge and minimize the negative impact of the domain-specific information. For instance, Tsai *et al.* [13] and Luo *et al.* [16] demand the generator to fool the discriminator on discriminating the feature from the source domain and target domain. Another line of works [24], [25], [17], [26], [27], [28] focuses on mining the domain-specific knowledge in the target domain. The main idea is to minimize the prediction entropy in the target domain [29], [30]. Zou *et al.* [24], [25] propose to leverage the pseudo labels with high confidence, and discuss different regularization terms. Taking one step further, Feng *et al.* [31] and Lin *et al.* [32] leverage the group information to acquire pseudo labels with high precision. leverage Zheng *et al.* [17] apply one two-step training strategy, which first conducts the domain alignment to generate better pseudo labels, and then apply the pseudo label learning. Furthermore, Zheng *et al.* [33] rectify the pseudo label learning by explicitly combining the prediction uncertainty into the cross-entropy loss. In this paper, we notice that existing works, to some extent, still suffer from over-fitting and early-stopping tricks, leading to large prediction variance and re-implementation difficulties. We propose an efficient bootstrapping method, which is orthogonal to most existing approaches on minimizing the domain gap. In fact,

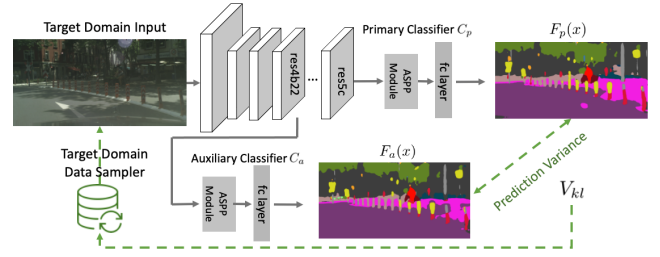


Fig. 2. Illustration of the basic model structure (Gray Parts). We follow most existing works [13], [15], [16], [14], [17], [33] to deploy the modified Deeplab-v2 [2] with ResNet-101 [42] as backbone. The auxiliary classifier is added to help the optimization, preventing gradient vanishment. In this work, we focus on the outer loop (Green Parts). We leverage the discrepancy of the segmentation outputs from the primary classifier C_p and C_a to acquire the prediction variance V_{kl} . The variance is then utilized to update the data sampler. More details can be found in Section III-A.

the proposed method can be fused with existing methods to further improve the model scalability.

B. Bootstrapping Learning

Bootstrapping learning denotes the capability of the model to progressively improve the performance by teaching itself [34]. The teacher-student training policy [35] is first proposed for model distillation, which intends to distill the knowledge from large-scale models to mobile models. It demands the parameter-efficient student model to predict consistent prediction scores with the large teacher model. However, teacher-student policy needs one pre-trained sophisticated network as the teacher model in advance, which is not always available. To address this limitation, Zhang *et al.* [36] introduce deep mutual learning to simultaneously train two models of different structures from scratch and learn from each other. Different from preserving two models during training, Laine *et al.* [37] propose Π model to enable the model learning from the model itself, which demands consistent prediction on the original input and the augmented input. Furthermore, Laine *et al.* also explore the temporal ensembling, which leverages the prediction history to stabilize the training. To address the out-of-the-date prediction in the history, Tarvainen *et al.* [38] and Choi *et al.* [39] propose to maintain one mean model by moving average weight [40], which does not need to train one new model again. Similarly, Chen *et al.* [41] and Zheng *et al.* [17] introduce the memory mechanism to help the feature update, facilitating the consistency learning. We are mainly different from existing bootstrapping learning approaches in two aspects: 1) We do not introduce more prerequisites, such as extra memory modules or an independent teacher model. Instead, we gradually aggregate the complementary model during training. The model can converge efficiently, and achieve competitive performance in the target domain quickly; 2) We explicitly consider the model weakness and adopt one adaptive data sampler, which focuses on the “hard” samples and facilitates learning complementary models in a coherent manner.

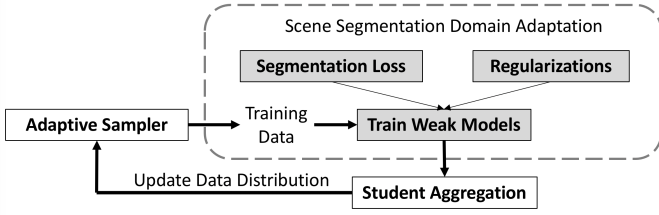


Fig. 3. The brief pipeline of the proposed method. There are two main components, *i.e.*, Adaptive Sampler and Student Aggregation. We modify the training data distribution to learn complementary “weak” models, preventing the model from over-fitting. **Different from existing methods, the pipeline enables interactions between learned models and the data sampler.** The proposed method is orthogonal to most existing scene segmentation domain adaptation approaches (in the rounded rectangle).

III. METHOD

Formulation. Given the labeled source-domain dataset $X_m = \{x_m^i\}_{i=1}^M$ and the unlabeled target-domain dataset $X_n = \{x_n^j\}_{j=1}^N$, scene segmentation domain adaptation is to learn the projection function F , which maps the input data X to the segmentation map Y . M and N denote the number of the source-domain images and the target-domain images, respectively. Following the common practise in [13], [15], [17], we adopt the modified DeepLabv2 [2] as the baseline model, which contains two classifiers, *i.e.*, the primary classifier C_p and the auxiliary classifier C_a . The auxiliary classifier design is to help optimization and prevent the gradient from vanishing. In this work, we also involve the auxiliary prediction into the calculation of the prediction variance V_{kl} . To simplify, we denote the two segmentation functions F_p and F_a , where $F_p(x)$ is the output of the primary classifier, and $F_a(x)$ is the output of the auxiliary classifier (see Figure 2).

Overview. In this work, we do not pursue a sophisticated segmentation structure or optimization losses. In contrast, we focus on the learning strategy. As shown in Figure 3, we provide one brief pipeline to illustrate the proposed approach, AdaBoost Student. AdaBoost Student contains two primary components, *i.e.*, Adaptive Sampler and Student Aggregation. Adaptive Sampler modifies the input training data distribution, and provides more emphasis on the uncertain samples. On the other hand, Student Aggregation is to accumulate the learned “weak” student models and output the prediction uncertainty to update data distribution. It is worth noting that there is one interaction loop from Adaptive Sampler to Student Aggregation, and back to Adaptive Sampler. We adopt one training policy similar to Generative Adversarial Network (GAN) [43]. During training, Student Aggregation updates the model parameters when the input data distribution is fixed, and vice versa. We fix the aggregated student model parameter to update the data distribution of Adaptive Sampler. We will illustrate the two components with details in the following sections.

A. Adaptive Sampler

Most bootstrapping works [34], [37] focus on mining the knowledge from the fixed data distribution, but ignore the attentions to the “hard” samples. The straightforward solution

underpinning the conventional method, *i.e.*, Adaptive boosting [18], is to improve the sampling rate of the wrong-classified samples. In a similar spirit, we adopt one adaptive sampler to progressively update the input data distribution D_t according to the epoch t . The initial data distribution $D_1(j) = 1/N$, and every sample has equal sampling probability. To learn the complementary models for the target domain, we improve the sampling rate of the “hard” target-domain samples with ambiguous predictions during training. It is worth noting that, due to the missing label in the target-domain, we can not deploy the prediction error to find the “hard” samples. Instead, we deploy the prediction variance as the “hard” indicator. Specifically, we formulate the prediction variance as the KL-divergence between the prediction of the primary classifier and the auxiliary classifier. The prediction variance of one single target-domain image can be calculated as:

$$V_{kl}(x_n^j|\theta) = \mathbb{E}[F_p(x_n^j|\theta) \log(\frac{F_p(x_n^j|\theta)}{F_a(x_n^j|\theta)})]. \quad (1)$$

If two classifiers predict the same class prediction, the value V_{kl} is low. Otherwise, the prediction variance is high, which indicates the model is not confident on such training data. In practise, since the output prediction is the pixel-wise segmentation map, we adopt the mean value of the whole prediction map as the indicator for the input image. To make V_{kl} as one distribution for the whole dataset, we apply the softmax function to normalize the prediction variance and make the sum of the V_{kl} equal to 1. The next data sampling distribution is averaged with the last data distribution and the normalized prediction variance as:

$$D_{t+1}(j) = \frac{1}{2}(D_t(j) + V_{kl}(x_n^j|\theta)). \quad (2)$$

Since $\sum_{j=1}^N D_t(j) = 1$ and $\sum_{j=1}^N V_{kl} = 1$, we ensure the update distribution $\sum_{j=1}^N D_{t+1} = 1$, and $D_{t+1}(j)$ is positive. As a result, the samples obtaining high prediction variance have more chances to be sampled in the next epoch.

Discussion. 1. Why is there a discrepancy between the primary classifier and the auxiliary classifier? It is mostly due to different receptive fields of two classifiers. Specifically, the input feature of the primary classifier is “res5c”, while the auxiliary classifier learns from the “res4b22” of the ResNet-101 backbone [42]. We leverage the prediction variance to represent the model uncertainty on the input data as [33]. Besides, we insert the dropout function before classifiers, which also enlarges the prediction discrepancy and helps to obtain the accurate uncertainty [44]. **2. What are the advantages of the proposed adaptive sampler?** There are two main points. First, we do not need the target-domain label to estimate the prediction error, which is different from the conventional AdaBoost algorithm in supervised learning. Instead, we leverage the prediction uncertainty to find the “hard” samples, which is more feasible for the domain adaptation problem. Second, existing methods usually ignore the importance of the input data distribution. The “easy” target-domain data, which has high prediction confidence, generally does not provide more domain-specific information about the target domain. The adaptive sampler explicitly introduces

the prediction variance into the data distribution update (see Eq. 2). We put more and more emphasis on the data with high uncertainty, facilitating the complementary model learning. The dynamic input distribution via the adaptive sampler encourages the knowledge transfer to the target domain efficiently. **3. Other sampling criterion.** Except the prediction variance, prediction entropy is another alternative choice. In the ablation study, we also provide the empirical result based on sampling criterion of the prediction entropy, which can be formulated as: $V_{en}(x_n^j|\theta) = \mathbb{E}[-F_p(x_n^j|\theta) \log(F_p(x_n^j|\theta))]$. A high value indicates that the prediction is close to the uniform distribution, and the model is not confident with the predicted classes given the input data. The samples obtaining high prediction entropy have more chances to be sampled in the next epoch. However, we observe one similar phenomenon with [33] that the prediction entropy is sensitive to the object edges in segmentation maps rather than the “hard” samples with ambiguous predictions, which needs to be “see” again. Therefore, the sampling criterion based on prediction entropy generally performs worse than the prediction variance in Eq. 1, which is verified in Table II.

B. Student Aggregation

In the conventional strategy, *i.e.*, Adaptive Boosting, multiple binary classifiers are sequentially learned with more attentions to the hard samples. Instead of training multiple deeply-learned models sequentially, we leverage the adaptive data sampler to enable learning complementary models in one-time training, which largely saves the training cost. Next we combine the vote of “weak” model snapshots as one final model. We regard snapshots as student models but do not introduce extra teachers. For the deeply-learned models, it is not efficient to preserve all the model snapshots in the memory, and fuse the prediction of every model, which demands the multiple-time inference. We follow Mean Teacher [38] to apply the weight average moving to keep one weight-averaged model of previous epochs:

$$\Theta_t = \sum \alpha_t \times \theta_t, \quad (3)$$

where the model weight α_t assigns different emphasis to “weak” models, and θ_t denotes the parameters of the student model at the t -th epoch. Θ_t denotes the parameters of the aggregated model. Since we can not foreknow the segmentation error on the target domain, we simply adopt average weights, which can be online updated as:

$$\Theta_t = \frac{t-1}{t} \Theta_{t-1} + \frac{1}{t} \theta_t, \quad (4)$$

where $t \in \{2, \dots, T_1\}$ and $\Theta_1 = \theta_1$. We do not need to update the mean student model very often. In our practise, we update the mean model every $T_2 = 5000$ iterations. **T_1 is the total training epoch number, while T_2 is the iteration number of each epoch.** We find that the weight averaging still can achieve a competitive result.

Discussion. 1. How about computation costs? *Time Cost.* As shown in Eq. 4, only 2 DNN weights need to be considered during every update, and the weight averaging costs about one forward inference time, which can be neglected [45].

Memory Cost. The main memory cost is to preserve one mean student model. We note that the mean student model can be moved to CPU memory during the idle time. We do not update the mean student model very often. When updating, we just move it back to GPU memory. Since we do not need to calculate the gradient but the mean of model parameters, the update process also costs limited memory. **2. What are the advantages of Student Aggregation?** The advantages are mostly in two aspects: First, instead of training $S(S > 5)$ classifiers in the conventional AdaBoost, we only need to keep one mean student model, which can be preserved in CPU memory. Second, the model update is efficient and effective, which does not require gradient calculation. We only need to update the weights of every layer to the mean value of existing snapshots. Meanwhile, student aggregation provides one final model with good generalizability, preventing from over-fitting as the traditional AdaBoost algorithm. More quantitative results are discussed in Experiment. **3. Correlation with Adaboost.** The main spirit of the proposed method is following Adaboost [18] to treat “hard” samples differently according to learned model snapshots. However, for domain adaptation, we can not foreknow the error e_m on the unlabeled target-domain data. Therefore, we adopt the trade-off. 1) In this work, we update the distribution based on the prediction variance instead of the error; 2) The binary classifier aggregation in Adaboost can be formulated as: $G(x) = \text{sign}(\sum_{m=1}^M \alpha_m G_m(x))$, where $G_m()$ is one of weak classifiers and α_m is the adaptive weights based on the error e_m . $\alpha_m = \frac{1}{2} \log(\frac{1-e_m}{e_m})$. Since the error e_m in target domain is unavailable, we deploy the temporal ensemble via weight averaging as a trade-off, which equals to set $\alpha_m = \frac{1}{M}$. In ablation studies, we also try different updating strategies, such as momentum, which is inferior to the proposed method. It verifies that the weight averaging trade-off is sub-optimal yet effective.

C. Optimization

We combine the two components, *i.e.*, adaptive sampler and student aggregation, in a coherent manner, and explicitly enable interactions between learned models and the data sampler. As shown in Algorithm 1, the adaptive sampler depends on the mean student model Θ_t to update the data distribution (see Eq. 8). Meanwhile, the adaptive sampler controls the input training data, which, in turn, affects the θ_t and Θ_t (see Eq. 7). Since we do not pursue new segmentation losses or regularization objectives, here we just mention the basic source-domain segmentation loss as:

$$L_{ce} = \mathbb{E}[-p_m^i \log F(x_m^i|\theta)]. \quad (9)$$

where p_m^i is the ground-truth probability vector of the label y_m^i . The value $p_m^i(c)$ equals to 1 if $c == y_m^i$ otherwise 0. Besides, there are multiple feasible regularization terms, including adversarial losses proposed in [13], [15] and consistency loss [17]. Without loss of generality, here we denote the regularization terms on the target domain as $R(x_n^j, \theta)$. Therefore, the optimization objective in every iteration can be formulated as:

$$L_{total} = L_{ce} + R(x_n^j, \theta). \quad (10)$$

Algorithm 1 Training Procedure of the Proposed Method

Require: The source domain dataset $X_m = \{X_m^i\}_{i=1}^M$; The source domain label $Y_m = \{y_m^i\}_{i=1}^M$; The unlabeled target domain dataset $X_n = \{x_n^j\}_{j=1}^N$;

Require: The source-domain parameter θ_s ; The epoch number T_1 ; The iteration number T_2 in each epoch.

- 1: Initialize $\theta = \theta_s$;
- 2: Initialize target domain data distribution $D_1(j) = 1/N$;
- 3: **for** epoch $t = 1$ to T_1 **do**
- 4: **for** iteration = 1 to T_2 **do**
- 5: To be simplify, here we only show the basic cross-entropy segmentation loss on the source domain data:

$$L_{ce} = \mathbb{E}[-p_m^i \log F(x_m^i | \theta)]. \quad (5)$$

- 6: We denotes other regularization losses on the target domain as $R(x_n^j, \theta)$. Update the model weight:

$$L_{total} = L_{ce} + R(x_n^j, \theta). \quad (6)$$

- 7: **end for**
- 8: $\theta_t = \theta$.
- 9: The mean model parameter is updated:

$$\Theta_t = \frac{t-1}{t} \Theta_{t-1} + \frac{1}{t} \theta_t. \quad (7)$$

- 10: Update the adaptive data distribution D_{t+1} :

$$D_{t+1}(j) = \frac{1}{2}(D_t(j) + V_{kl}(x_n^j | \Theta_t)), \quad (8)$$

where V_{kl} is the prediction variance defined in Eq. 1, and we apply the current mean model Θ_t to estimate the variance.

- 11: **end for**
- 12: **return** Θ_t .

After every T_2 iterations, we update the adaptive sampler and the mean student model, as discussed in the Section III-A and Section III-B. The training is stopped after T_1 epochs.

IV. EXPERIMENT

A. Implementation Details

Network Architecture. We adopt the Deeplab-v2 [2] as the baseline model, which deploys the ResNet-101 [42] as backbone. Following most existing works [13], [14], [15], [16], [17], [33], we insert one auxiliary classifier with the same structure as the primary classifier. The classifier consists of one Atrous Spatial Pyramid Pooling (ASPP) module [2] and one fully-connected layer. The auxiliary classifier is added at the *res4b22* layer. We also insert the dropout layer of 0.2 drop rate before the fully-connected layer.

Training Details. Following existing works [13], [15], the input image is resized to 1280×640 , and we randomly crop 1024×512 for training. Random horizontal flipping is also applied. We deploy the SGD optimizer with a mini-batch of 2. The initial learning rate is set as 0.0002. Following [1], [46], [47], we deploy the ploy learning rate policy by multiplying the scale factor $(1 - \frac{\text{current_iter}}{\text{total_iter}})^{0.9}$. The total iteration is set as 50k ($T_1 = 10, T_2 = 5000$). When inference, we follow [17], [33] to combine the prediction of the two classifiers as the final prediction. Our implementation is based on Pytorch [48].

TABLE I

LIST OF CATEGORIES AND NUMBER OF IMAGES OF FOUR DATASETS, *i.e.*, GTA5 [5], SYNTHIA [49], CITYSCAPES [6] AND OXFORD ROBOTCAR [50].

Datasets	GTA5	SYNTHIA	Cityscapes	Oxford RobotCar
#Train Images	24,966	9,400	2,975	894
#Test Images	-	-	500	271
#Category	19	16	19	9
Synthetic	✓	✓	×	×

B. Datasets and Evaluation Metric

Datasets. In this work, we conduct experiments on three scene segmentation domain adaptation benchmarks. To simplify the illustration, we denote the source dataset A and the target dataset B as $A \rightarrow B$. Two widely-used benchmarks are to leverage the synthetic data to learn the shared knowledge, and adapt the knowledge to the real-world scenario. The settings are GTA5 [5] \rightarrow Cityscapes [6] and SYNTHIA [49] \rightarrow Cityscapes [6]. In particular, the GTA5 dataset is collected from one video game, which contains 24,966 labeled image for training. The SYNTHIA dataset is generated from a virtual city engine with pixel-level annotations as well, including 9,400 training images. The target dataset, *i.e.*, Cityscapes, collects the real-world street-view images from 50 different cities, yielding 2,975 unlabeled training images and 500 images for testing. We also adopt one cross-city benchmark, *i.e.*, Cityscapes [6] \rightarrow Oxford RobotCar [50]. In this setting, we use the annotation of 2,975 training images of the Cityscapes dataset. In contrast with the Synthetic-to-real setting, the Oxford RobotCar dataset is also collected from the realistic street-view camera. The challenge is in the noisy variants, such as weather and illumination conditions. The Oxford RobotCar dataset is collected in rainy days and cloudy days, while the Cityscapes dataset mostly contains images in sunny days. More details are shown in Table I.

Evaluation Metric. We follow previous works to report the IoU accuracy of each category, and mean IoU (mIoU) for all the classes. For SYNTHIA \rightarrow Cityscapes, some previous works report the mean IoU over 13 classes, while others report both 13 classes and 16 classes. We report both results, and denote the results of 13 classes and 16 classes as mIoU* and mIoU, respectively. For GTA5 \rightarrow Cityscapes and Cityscapes \rightarrow Oxford RobotCar, we report the 19-category and 9-category accuracy, respectively.

C. Ablation Studies

Effect of the Adaptive Sampler. First, we study the adaptive sampler. Since we intend to learn the complementary model snapshots, as shown in Table II, the single “weak” model does not achieve significant improvement, even with the performance drop. The observation is aligned with the conventional AdaBoost algorithm [18], since the current snapshot takes more attention to “hard” samples. Compared with the baseline method, *i.e.*, MRNet [17], which achieves 45.5% mIoU accuracy, the MRNet using adaptive sampler decreases to 45.2%. It is because the hard negatives do not lead

TABLE II

ABLATION STUDY OF THE TWO COMPONENTS IN ADABOOST STUDENT ON GTA5→CITYSCAPES. WE ADOPT THE MRNET [17] AS BASELINE, AND STUDY THE IMPACT OF THE ADAPTIVE SAMPLER AND THE STUDENT AGGREGATION ALONE. THE RESULTS SUGGEST THAT THE ADAPTIVE SAMPLER DOES NOT IMPROVE THE SINGLE MODEL PERFORMANCE BUT HELPS COMPLEMENTARY MODEL LEARNING, FACILITATING THE FINAL “WEAK” STUDENT MODEL AGGREGATION. OURS (ENTROPY) DENOTES THAT WE APPLY THE PREDICTION ENTROPY TO UPDATE THE ADAPTIVE SAMPLER, WHILE OURS (VARIANCE) IS THE DEFAULT SETTING IF NOT SPECIFIED.

Method	Student Aggregation	Adaptive Sampler	mIoU
MRNet [17]			45.5
w Adaptive Sampler		✓	45.2
w Student Aggregation	✓		48.4
MRNet [17] + Ours (entropy)	✓	✓	48.1
MRNet [17] + Ours (variance)	✓	✓	49.0

to one single optimal student model but the complementary model of the last model snapshot. If we further apply the student aggregation, MRNet + Ours has achieved significant improvement from 45.2% mIoU accuracy to 49.0% mIoU accuracy, which also surpasses MRNet (45.5% mIoU) by a relatively large margin. By default, we apply the sampler based on the prediction variance, and we observe that the alternative sampler based on the prediction entropy leads to one inferior performance of 48.1% mIoU. It is mainly due to the prediction entropy takes more attention to the object edges as showed in [33], which can not nominate “hard” samples with ambiguous predictions accurately.

Effect of the Student Aggregation. We also investigate the student aggregation in Adaboost Student (see Table II). There are two main observations. (1) The student aggregation alone can yield the performance improvement. It is due to the model discrepancy during training. Especially for the scene segmentation, the extreme small training batch sizes and data shuffle lead to different training order in every epoch. Therefore, the baseline method, *i.e.*, MRNet, with student aggregation alone, has arrived at 48.4% mIoU accuracy from 45.5% mIoU. (2) Since the input data distribution is fixed in the baseline method, the model snapshots are still homogeneous due to the training data. In contrast, the proposed method explicitly demands learning complementary models by the dynamic input data via the adaptive sampler. The full method with the adaptive sampler, therefore, yields better results at 49.0%, surpassing the student aggregation alone (48.4%). The results also suggest the effectiveness of the adaptive sampler.

Compatibility of the Proposed Method. We argue that the proposed method is orthogonal to most existing methods, and can be fused with existing frameworks to obtain better performance. Therefore, we re-implement three existing approaches, including AdaptSegNet [13], MRNet [17] and Uncertainty [33]. As shown in Table III, we observe one consistent performance improvement on GTA5→Cityscapes for all three methods. For the widely-adopted method, *i.e.*, AdaptSegNet [13], AdaptSegNet + Ours has arrived at 47.3% mIoU, which surpasses the original AdaptSegNet (42.4%) by +4.9%. Furthermore, we observe one similar performance improvement on recent methods. MRNet [17] + Ours has boosted

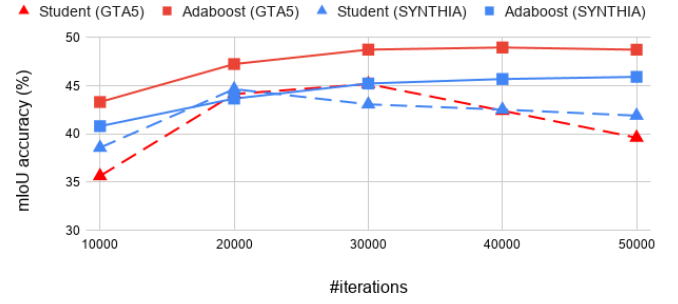


Fig. 4. Convergence of the proposed method. We provide the sensitivity analysis of MRNet+Ours on two benchmarks, *i.e.*, GTA5→Cityscapes (GTA5) and SYNTHIA→Cityscapes (SYNTHIA). The results suggest that the AdaBoost Student model (AdaBoost) quickly converges, while the performance of the student model (Student) is still fluctuating.

from 45.5% mIoU accuracy to 49.0%, while Uncertainty [33] + Ours obtains +0.6% from 50.3% to 50.9% mIoU accuracy. As shown in Table IV and Table V, we observe one similar result on both SYNTHIA→Cityscapes and Cityscapes→Oxford RobotCar benchmarks. For the SYNTHIA→Cityscapes benchmark, AdaptSegNet [13], MRNet [17] and Uncertainty [33] have achieved +1.2%, +2.7% and +2.6% mIoU*, respectively. On the other hand, AdaptSegNet [13], MRNet [17] and Uncertainty [33] have achieved +1.8%, +1.2% and +0.8% mIoU on the Cityscapes→Oxford RobotCar benchmark, respectively. In a summary, the extensive experiment with three methods on three benchmarks verifies that the proposed approach, Adaptive Student, can be fused with existing frameworks to improve the model generalizability in the target domain.

Limitation. We observe that the proposed method shows less improvement on the pseudo label learning based method, *i.e.*, Uncertainty [33] than the domain alignment based method, *i.e.*, AdaptSegNet [13] and MRNet [17]. The main reason is the strong supervised learning of the generated pseudo labels on the target domain, which limits the model discrepancy and compromises learning complementary “weak” models in the proposed AdaBoost Student.

Convergence of the Proposed Method. One advantage of the proposed method is the quick convergence to one robust model after limited iterations, since the complementary models are aggregated during training. Here we provide the sensitivity analysis of convergence time on both GTA5 → Cityscapes and SYNTHIA → Cityscapes. We adopt MRNet as the baseline model. As shown in Figure 4, we observe that the proposed method can efficiently converge at around 30,000 iterations, while the student models are still jittering during training.

D. Comparisons with State-of-the-art Methods

Synthetic-to-real. We mainly compare other recent methods on two synthetic-to-real benchmarks, which leverage the synthetic data to learn the shared knowledge. We compare recent methods with reported results as well as several methods re-implemented by us. For a fair comparison, we compare models with a similar structure, which is based on the Deeplab-v2 [2],

TABLE III

QUANTITATIVE RESULTS ON GTA5 \rightarrow CITYSCAPES. WE PRESENT PRE-CLASS IOU AND MIOU. THE BEST ACCURACY IN EVERY COLUMN IS IN **BOLD**.

Method	Road	SW	Build	Wall	Fence	Pole	TL	TS	Veg.	Terrain	Sky	PR	Rider	Car	Truck	Bus	Train	Motor	Bike	mIoU
Source	75.8	16.8	77.2	12.5	21.0	25.5	30.1	20.1	81.3	24.6	70.3	53.8	26.4	49.9	17.2	25.9	6.5	25.3	36.0	36.6
AdaptSegNet [13]	86.5	36.0	79.9	23.4	23.3	23.9	35.2	14.8	83.4	33.3	75.6	58.5	27.6	73.7	32.5	35.4	3.9	30.1	28.1	42.4
AdaptSegNet [13] + Ours	89.5	34.1	83.7	31.5	25.0	36.0	40.6	34.6	85.6	44.6	77.8	61.4	30.4	85.6	35.9	47.1	1.8	19.4	34.1	47.3
SIBAN [15]	88.5	35.4	79.5	26.3	24.3	28.5	32.5	18.3	81.2	40.0	76.5	58.1	25.8	82.6	30.3	34.4	3.4	21.6	21.5	42.6
CLAN [16]	87.0	27.1	79.6	27.3	23.3	28.3	35.5	24.2	83.6	27.4	74.2	58.6	28.0	76.2	33.1	36.7	6.7	31.9	31.4	43.2
SP-Adv [51]	86.2	38.4	80.8	25.5	20.5	32.8	33.4	28.2	85.5	36.1	80.2	60.3	28.6	78.7	27.3	36.1	4.6	31.6	28.4	44.3
MaxSquare [52]	88.1	27.7	80.8	28.7	19.8	24.9	34.0	17.8	83.6	34.7	76.0	58.6	28.6	84.1	37.8	43.1	7.2	32.3	34.2	44.3
ASA [53]	89.2	27.8	81.3	25.3	22.7	28.7	36.5	19.6	83.8	31.4	77.1	59.2	29.8	84.3	33.2	45.6	16.9	34.5	30.8	45.1
APODA [54]	85.6	32.8	79.0	29.5	25.5	26.8	34.6	19.9	83.7	40.6	77.9	59.2	28.3	84.6	34.6	49.2	8.0	32.6	39.6	45.9
PatchAlign [14]	92.3	51.9	82.1	29.2	25.1	24.5	33.8	33.0	82.4	32.8	82.2	58.6	27.2	84.3	33.4	46.3	2.2	29.5	32.3	46.5
BL [27]	91.0	44.7	84.2	34.6	27.6	30.2	36.0	36.0	85.0	43.6	83.0	58.6	31.6	83.3	35.3	49.7	3.3	28.8	35.6	48.5
DT [55]	90.6	44.7	84.8	34.3	28.7	31.6	35.0	37.6	84.7	43.3	85.3	57.0	31.5	83.8	42.6	48.5	1.9	30.4	39.0	49.2
AdvEnt [56]	89.4	33.1	81.0	26.6	26.8	27.2	33.5	24.7	83.9	36.7	78.8	58.7	30.5	84.8	38.5	44.5	1.7	31.6	32.4	45.5
Source	-	-	-	-	-	-	-	-	-	-	-	-	-	-	-	-	-	-	-	29.2
FCAN [57]	-	-	-	-	-	-	-	-	-	-	-	-	-	-	-	-	-	-	-	46.6
Source	71.3	19.2	69.1	18.4	10.0	35.7	27.3	6.8	79.6	24.8	72.1	57.6	19.5	55.5	15.5	15.1	11.7	21.1	12.0	33.8
CBST [24]	91.8	53.5	80.5	32.7	21.0	34.0	28.9	20.4	83.9	34.2	80.9	53.1	24.0	82.7	30.3	35.9	16.0	25.9	42.8	45.9
MRKLD [25]	91.0	55.4	80.0	33.7	21.4	37.3	32.9	24.5	85.0	34.1	80.8	57.7	24.6	84.1	27.8	30.1	26.9	26.0	42.3	47.1
Source	51.1	18.3	75.8	18.8	16.8	34.7	36.3	27.2	80.0	23.3	64.9	59.2	19.3	74.6	26.7	13.8	0.1	32.4	34.0	37.2
MRNet [17]	89.1	23.9	82.2	19.5	20.1	33.5	42.2	39.1	85.3	33.7	76.4	60.2	33.7	86.0	36.1	43.3	5.9	22.8	30.8	45.5
MRNet [17] + Ours	89.5	36.6	84.8	37.9	29.8	37.9	45.1	34.9	85.8	43.6	80.4	64.7	35.3	84.9	30.4	45.9	2.7	24.7	35.7	49.0
Uncertainty [33]	90.4	31.2	85.1	36.9	25.6	37.5	48.8	48.5	85.3	34.8	81.1	64.4	36.8	86.3	34.9	52.2	1.7	29.0	44.6	50.3
Uncertainty [33] + Ours	90.7	35.9	85.7	40.1	27.8	39.0	49.0	48.4	85.9	35.1	85.1	63.1	34.4	86.8	38.3	49.5	0.2	26.5	45.3	50.9

TABLE IV

QUANTITATIVE RESULTS ON SYNTHIA \rightarrow CITYSCAPES. WE PRESENT PRE-CLASS IOU, MIOU AND MIOU*. MIOU AND MIOU* ARE AVERAGED OVER 16 AND 13 CATEGORIES, RESPECTIVELY. THE BEST ACCURACY IN EVERY COLUMN IS IN **BOLD**.

Method	Road	SW	Build	Wall*	Fence*	Pole*	TL	TS	Veg.	Sky	PR	Rider	Car	Bus	Motor	Bike	mIoU*	mIoU
Source	55.6	23.8	74.6	—	—	—	6.1	12.1	74.8	79.0	55.3	19.1	39.6	23.3	13.7	25.0	38.6	—
MaxSquare [52]	77.4	34.0	78.7	5.6	0.2	27.7	5.8	9.8	80.7	83.2	58.5	20.5	74.1	32.1	11.0	29.9	45.8	39.3
SIBAN [15]	82.5	24.0	79.4	—	—	—	16.5	12.7	79.2	82.8	58.3	18.0	79.3	25.3	17.6	25.9	46.3	—
PatchAlign [14]	82.4	38.0	78.6	8.7	0.6	26.0	3.9	11.1	75.5	84.6	53.5	21.6	71.4	32.6	19.3	31.7	46.5	40.0
AdaptSegNet [13]	84.3	42.7	77.5	—	—	—	4.7	7.0	77.9	82.5	54.3	21.0	72.3	32.2	18.9	32.3	46.7	—
AdaptSegNet [13] + Ours	67.9	30.1	77.9	10.2	1.5	37.2	30.9	22.3	80.8	83.1	52.4	20.9	72.9	25.4	12.7	45.7	47.9	42.0
CLAN [16]	81.3	37.0	80.1	—	—	—	16.1	13.7	78.2	81.5	53.4	21.2	73.0	32.9	22.6	30.7	47.8	—
SP-Adv [51]	84.8	35.8	78.6	—	—	—	6.2	15.6	80.5	82.0	66.5	22.7	74.3	34.1	19.2	27.3	48.3	—
ASA [53]	91.2	48.5	80.4	3.7	0.3	21.7	5.5	5.2	79.5	83.6	56.4	21.0	80.3	36.2	20.0	32.9	49.3	41.7
DADA [9]	89.2	44.8	81.4	6.8	0.3	26.2	8.6	11.1	81.8	84.0	54.7	19.3	79.7	40.7	14.0	38.8	49.8	42.6
BL [27]	86.0	46.7	80.3	—	—	—	14.1	11.6	79.2	81.3	54.1	27.9	73.7	42.2	25.7	45.3	51.4	—
DT [55]	83.0	44.0	80.3	—	—	—	17.1	15.8	80.5	81.8	59.9	33.1	70.2	37.3	28.5	45.8	52.1	—
CCM [58]	79.6	36.4	80.6	13.3	0.3	25.5	22.4	14.9	81.8	77.4	56.8	25.9	80.7	45.3	29.9	52.0	52.9	45.2
APODA [54]	86.4	41.3	79.3	—	—	—	22.6	17.3	80.3	81.6	56.9	21.0	84.1	49.1	24.6	45.7	53.1	—
AdvEnt [56]	85.6	42.2	79.7	8.7	0.4	25.9	5.4	8.1	80.4	84.1	57.9	23.8	73.3	36.4	14.2	33.0	48.0	41.2
Source	64.3	21.3	73.1	2.4	1.1	31.4	7.0	27.7	63.1	67.6	42.2	19.9	73.1	15.3	10.5	38.9	40.3	34.9
CBST [24]	68.0	29.9	76.3	10.8	1.4	33.9	22.8	29.5	77.6	78.3	60.6	28.3	81.6	23.5	18.8	39.8	48.9	42.6
MRKLD [25]	67.7	32.2	73.9	10.7	1.6	37.4	22.2	31.2	80.8	80.5	60.8	29.1	82.8	25.0	19.4	45.3	50.1	43.8
Source	44.0	19.3	70.9	8.7	0.8	28.2	16.1	16.7	79.8	81.4	57.8	19.2	46.9	17.2	12.0	43.8	40.4	35.2
MRNet [17]	82.0	36.5	80.4	4.2	0.4	33.7	18.0	13.4	81.1	80.8	61.3	21.7	84.4	32.4	14.8	45.7	50.2	43.2
MRNet [17] + Ours	83.6	40.1	81.3	9.6	0.8	36.8	25.8	16.3	84.5	87.1	60.3	23.9	84.9	32.3	19.0	48.4	52.9	45.9
Uncertainty [33]	87.6	41.9	83.1	14.7	1.7	36.2	31.3	19.9	81.6	80.6	63.0	21.8	86.2	40.7	23.6	53.1	54.9	47.9
Uncertainty [33] + Ours	85.6	43.9	83.9	19.2	1.7	38.0	37.9	19.6	85.5	88.4	64.1	25.7	86.6	43.9	31.2	51.3	57.5	50.4

TABLE V

QUANTITATIVE RESULTS ON THE CROSS-CITY BENCHMARK: CITYSCAPES \rightarrow OXFORD ROBOTCAR. THE BEST ACCURACY IN EVERY COLUMN IS IN **BOLD**.

Method	road	sidewalk	building	light	sign	sky	person	automobile	two-wheel	mIoU
Source	79.2	49.3	73.1	55.6	37.3	36.1	54.0	81.3	49.7	61.9
AdaptSegNet [13]	95.1	64.0	75.7	61.3	35.5	63.9	58.1	84.6	57.0	69.5
AdaptSegNet [13] + Ours	96.0	73.0	91.5	65.8	22.9	94.9	56.0	89.0	53.0	71.3
PatchAlign [14]	94.4	63.5	82.0	61.3	36.0	76.4	61.0	86.5	58.6	72.0
MRNet [17]	95.9	73.5	86.2	69.3	31.9	87.3	57.9	88.8	61.5	72.5
MRNet [17] + Ours	96.4	77.0	83.4	70.7	39.2	83.0	62.4	89.9	61.0	73.7
Uncertainty [33]	95.9	73.7	87.4	72.8	43.1	88.6	61.7	89.6	57.0	74.4
Uncertainty [33] + Ours	96.1	75.3	92.1	72.6	37.0	94.4	62.7	89.7	56.9	75.2

and the backbone is ResNet-101 [42]. The competitive methods can be generally classified into two categories according to the usage of the pseudo label. One line of works focuses on the domain alignment, including AdaptSegNet [13], SIBAN [15], CLAN [16], APODA [54], PatchAlign [14], DT [55] and

MRNet [17]. Another line of works focuses on mining the target-domain knowledge via noisy labels and deploys the pseudo label learning, such as CBST [24], MRKLD [25] and Uncertainty [33], which generally achieves higher performance. As shown in Table III and Table IV, the proposed method yields consistent improvement in both kinds of works. The competitive performance has been achieved by combining AdaBoost Student with the Uncertainty [33]. Specifically, we have achieved 50.9% and 50.4% mIoU accuracy on GTA5 \rightarrow Cityscapes and SYNTHIA \rightarrow Cityscapes, respectively. Furthermore, the pre-class IoU results also suggest that the proposed method has achieved relatively good results on several classes of small-scale objectives, including Pole, Wall, and Fence.

Cross-city. We also evaluate the proposed method on one new cross-city benchmarks, *i.e.*, Cityscapes \rightarrow Oxford RobotCar (see Table V). Both Cityscapes and Oxford RobotCar are

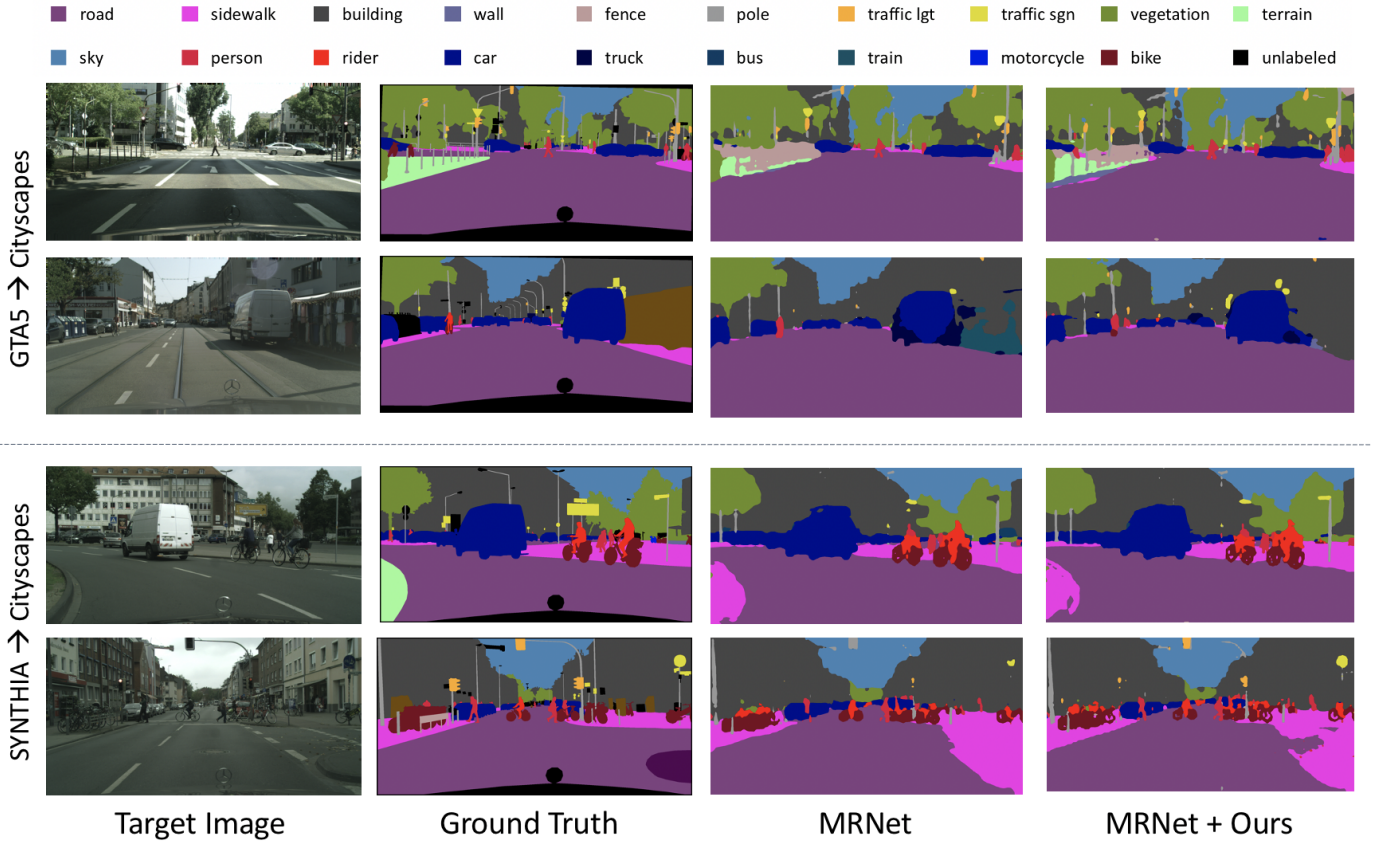


Fig. 5. Qualitative results of semantic segmentation adaptation on GTA5 \rightarrow Cityscapes and SYNTHIA \rightarrow Cityscapes. We show the original target-domain image, the ground-truth segmentation, the output of methods, *i.e.*, MRNet [17], and MRNet [17] + Ours. Our results are in the right column. (Best viewed in color).

collected from the realistic scenarios but in different cities and weather. The proposed method also has achieved the competitive result of 75.2% mIoU accuracy and showed a consistent performance improvement with other existing methods.

Qualitative Results. Furthermore, we provide the segmentation results in Figure 5, which also verifies the effectiveness of the proposed method. Comparing to the segmentation predictions of vanilla MRNet [17], the MRNet + Ours generally rectifies the object details, and achieves more robust outputs on the target domain.

V. FURTHER ANALYSIS AND DISCUSSIONS

Network Structure. We also verify the proposed method on a relatively vanilla network, *i.e.*, VGG16 [59]. Following previous works, we do not introduce BN (Batch Normalization) layers in the backbone network. We re-implement the MRNet [17], which has achieved 25.5% mIoU on GTA5 \rightarrow Cityscapes. As shown in Table VI, we can observe two main points. First, the proposed method is complementary to the existing works, *e.g.*, MRNet [17], and the MRNet [17] + Ours achieves +14.0% mIoU improvements. Second, we also achieve one competitive result 39.5% mIoU with other existing methods based on VGG16.

Aggregation with Momentum. Due to the prediction fluctuation on the target domain, we can not foreknow which snap-

TABLE VI
ABLATION STUDY ON THE EFFECTIVENESS OF THE PROPOSED METHOD ON A RELATIVELY VANILLA NETWORK, *i.e.*, VGG16 [59] ON GTA5 \rightarrow CITYSCAPES. *: WE RE-IMPLEMENT MRNET [17] WITH VGG16.

Method	Backbone	mIoU
Curriculum DA [60]	VGG16	28.9
Wang <i>et al.</i> [61]	VGG19	33.1
CyCADA [10]	VGG16	35.4
ASA [53]	VGG16	35.6
CBST-SP [24]	VGG16	36.1
DCAN [11]	VGG16	36.2
SP-Adv [51]	VGG16	36.5
MRNet* [17]	VGG16	25.5
MRNet* [17] + Ours	VGG16	39.5

shot is reliable. We also run MRNet+Ours with momentum strategy [62] on GTA5 \rightarrow Cityscapes. Two momentum values 0.9 and 0.5 are explored to keep old weights. The aggregated model only achieves 46.4% and 45.3%, respectively, which is inferior to the weight averaging. It verifies that the weight averaging trade-off is sub-optimal yet effective. In this paper, we leverage the weight averaging strategy, but it is still open to other aggregation alternatives.

vs. Mean Teacher (MT). Similarly, the existing method, *i.e.*, Mean Teacher (MT) [38] also preserves one weight-average model during the training process. We apply the same

strategy, including iteration numbers, to update the teacher model and re-implement Mean Teacher. The main difference between the proposed method and Mean Teacher (MT) are two points: First, we adopt the adaptive sampler, which enables interactions between learned models and the data sampler. In this way, the proposed method leads to more complementary snapshots during training for the student aggregation. Second, Mean Teacher needs the teacher prediction in every iteration. It demands extra model inference to calculate the kl-divergence loss (costs extra time and memory), and forces the student model and the weight-average teacher model to predict the same distribution given the input, which also limits learning complementary student models. In contrast, the proposed method does not introduce such an objective and performs more efficiently and effectively with the spirit of AdaBoost [18]. As a result, the proposed method outperforms MT (Student) 46.6% and MT (Teacher) 47.5% mIoU (see Table VII).

TABLE VII
COMPARISON WITH MEAN TEACHER (MT) [38].

Method	mIoU
MRNet [17]	45.5
MRNet [17] + MT (Student)	46.6
MRNet [17] + MT (Teacher)	47.5
MRNet [17] + Ours	49.0

VI. CONCLUSION

We identify one practical challenge in deciding the early-stopping time of the scene segmentation domain adaptation task. To address this limitation, we propose an efficient bootstrapping solution, AdaBoost Student, to learn the scalable model by aggregating “weak” models. The main idea underpinning AdaBoost Student is to leverage the model discrepancy during training. Specifically, AdaBoost Student adopts one adaptive data sampler and explicitly facilitates learning complementary models in a coherent manner. Thus, AdaBoost Student can efficiently converge to one robust final model and prevent over-fitting. As a result, we have achieved consistent improvements and competitive results on three benchmarks, including two synthetic-to-real benchmarks and one cross-city benchmark. In the future, we will continue to investigate the usage of Adaboost Student and apply it to other fields, such as medical images, to obtain the model with good generalizability.

REFERENCES

- [1] H. Zhao, J. Shi, X. Qi, X. Wang, and J. Jia, “Pyramid scene parsing network,” in *CVPR*, 2017.
- [2] L.-C. Chen, G. Papandreou, I. Kokkinos, K. Murphy, and A. L. Yuille, “Deeplab: Semantic image segmentation with deep convolutional nets, atrous convolution, and fully connected crfs,” *IEEE transactions on pattern analysis and machine intelligence*, vol. 40, no. 4, pp. 834–848, 2017.
- [3] Z. Wu, X. Wang, J. E. Gonzalez, T. Goldstein, and L. S. Davis, “Ace: adapting to changing environments for semantic segmentation,” in *ICCV*, 2019.
- [4] Y. Pan, T. Yao, Y. Li, Y. Wang, C.-W. Ngo, and T. Mei, “Transferrable prototypical networks for unsupervised domain adaptation,” in *CVPR*, 2019.

- [5] S. R. Richter, V. Vineet, S. Roth, and V. Koltun, “Playing for data: Ground truth from computer games,” in *ECCV*, 2016.
- [6] M. Cordts, M. Omran, S. Ramos, T. Rehfeld, M. Enzweiler, R. Benenson, U. Franke, S. Roth, and B. Schiele, “The cityscapes dataset for semantic urban scene understanding,” in *CVPR*, 2016.
- [7] Y. Chen, W. Li, X. Chen, and L. V. Gool, “Learning semantic segmentation from synthetic data: A geometrically guided input-output adaptation approach,” in *CVPR*, 2019.
- [8] Y.-C. Chen, Y.-Y. Lin, M.-H. Yang, and J.-B. Huang, “Crdoco: Pixel-level domain transfer with cross-domain consistency,” in *CVPR*, 2019.
- [9] T.-H. Vu, H. Jain, M. Bucher, M. Cord, and P. Pérez, “Dada: Depth-aware domain adaptation in semantic segmentation,” in *ICCV*, 2019.
- [10] J. Hoffman, E. Tzeng, T. Park, J.-Y. Zhu, P. Isola, K. Saenko, A. A. Efros, and T. Darrell, “Cycada: Cycle-consistent adversarial domain adaptation,” in *ICML*, 2018.
- [11] Z. Wu, X. Han, Y.-L. Lin, M. Gokhan Uzunbas, T. Goldstein, S. Nam Lim, and L. S. Davis, “Dcan: Dual channel-wise alignment networks for unsupervised scene adaptation,” in *ECCV*, 2018.
- [12] B. Geng, D. Tao, and C. Xu, “Daml: Domain adaptation metric learning,” *IEEE Transactions on Image Processing*, vol. 20, no. 10, pp. 2980–2989, 2011.
- [13] Y.-H. Tsai, W.-C. Hung, S. Schuster, K. Sohn, M.-H. Yang, and M. Chandraker, “Learning to adapt structured output space for semantic segmentation,” in *CVPR*, 2018.
- [14] Y.-H. Tsai, K. Sohn, S. Schuster, and M. Chandraker, “Domain adaptation for structured output via discriminative representations,” in *ICCV*, 2019.
- [15] Y. Luo, P. Liu, T. Guan, J. Yu, and Y. Yang, “Significance-aware information bottleneck for domain adaptive semantic segmentation,” in *ICCV*, 2019.
- [16] Y. Luo, L. Zheng, T. Guan, J. Yu, and Y. Yang, “Taking a closer look at domain shift: Category-level adversaries for semantics consistent domain adaptation,” in *CVPR*, 2019.
- [17] Z. Zheng and Y. Yang, “Unsupervised scene adaptation with memory regularization in vivo,” in *IJCAI*, 2020.
- [18] Y. Freund, R. E. Schapire *et al.*, “Experiments with a new boosting algorithm,” in *ICML*, 1996.
- [19] Y. Luo, P. Liu, T. Guan, J. Yu, and Y. Yang, “Adversarial style mining for one-shot unsupervised domain adaptation,” in *NeurIPS*, 2020.
- [20] R. Gong, W. Li, Y. Chen, and L. V. Gool, “Dlow: Domain flow for adaptation and generalization,” in *CVPR*, 2019.
- [21] L. Du, J. Tan, H. Yang, J. Feng, X. Xue, Q. Zheng, X. Ye, and X. Zhang, “Ssf-dan: Separated semantic feature based domain adaptation network for semantic segmentation,” in *ICCV*, 2019.
- [22] J.-Y. Zhu, T. Park, P. Isola, and A. A. Efros, “Unpaired image-to-image translation using cycle-consistent adversarial networks,” in *ICCV*, 2017.
- [23] X. Yue, Y. Zhang, S. Zhao, A. Sangiovanni-Vincentelli, K. Keutzer, and B. Gong, “Domain randomization and pyramid consistency: Simulation-to-real generalization without accessing target domain data,” in *ICCV*, 2019.
- [24] Y. Zou, Z. Yu, B. Vijaya Kumar, and J. Wang, “Unsupervised domain adaptation for semantic segmentation via class-balanced self-training,” in *ECCV*, 2018.
- [25] Y. Zou, Z. Yu, X. Liu, B. Kumar, and J. Wang, “Confidence regularized self-training,” in *ICCV*, 2019.
- [26] Q. Zhou, Z. Feng, G. Cheng, X. Tan, J. Shi, and L. Ma, “Uncertainty-aware consistency regularization for cross-domain semantic segmentation,” *arXiv:2004.08878*, 2020.
- [27] Y. Li, L. Yuan, and N. Vasconcelos, “Bidirectional learning for domain adaptation of semantic segmentation,” in *Proceedings of the IEEE/CVF Conference on Computer Vision and Pattern Recognition*, 2019, pp. 6936–6945.
- [28] P. Zhang, B. Zhang, T. Zhang, D. Chen, Y. Wang, and F. Wen, “Prototypical pseudo label denoising and target structure learning for domain adaptive semantic segmentation,” in *CVPR*, 2021.
- [29] Y. Huang, J. Xu, Q. Wu, Z. Zheng, Z. Zhang, and J. Zhang, “Multi-pseudo regularized label for generated data in person re-identification,” *IEEE Transactions on Image Processing*, vol. 28, no. 3, pp. 1391–1403, 2018.
- [30] G. Ding, S. Zhang, S. Khan, Z. Tang, J. Zhang, and F. Porikli, “Feature affinity-based pseudo labeling for semi-supervised person re-identification,” *IEEE Transactions on Multimedia*, vol. 21, no. 11, pp. 2891–2902, 2019.
- [31] H. Feng, M. Chen, J. Hu, D. Shen, H. Liu, and D. Cai, “Complementary pseudo labels for unsupervised domain adaptation on person re-identification,” *IEEE Transactions on Image Processing*, vol. 30, pp. 2898–2907, 2021.

- [32] Y. Lin, L. Xie, Y. Wu, C. Yan, and Q. Tian, "Unsupervised person re-identification via softened similarity learning," in *Proceedings of the IEEE/CVF Conference on Computer Vision and Pattern Recognition*, 2020, pp. 3390–3399.
- [33] Z. Zheng and Y. Yang, "Rectifying pseudo label learning via uncertainty estimation for domain adaptive semantic segmentation," *International Journal of Computer Vision (IJCV)*, 2020, doi:[10.1007/s11263-020-01395-y](https://doi.org/10.1007/s11263-020-01395-y).
- [34] S. Reed, H. Lee, D. Anguelov, C. Szegedy, D. Erhan, and A. Rabinovich, "Training deep neural networks on noisy labels with bootstrapping," in *ICLR workshop*, 2014.
- [35] G. Hinton, O. Vinyals, and J. Dean, "Distilling the knowledge in a neural network," in *NeurIPS*, 2015.
- [36] Y. Zhang, T. Xiang, T. M. Hospedales, and H. Lu, "Deep mutual learning," in *CVPR*, 2018.
- [37] S. Laine and T. Aila, "Temporal ensembling for semi-supervised learning," in *ICLR*, 2016.
- [38] A. Tarvainen and H. Valpola, "Mean teachers are better role models: Weight-averaged consistency targets improve semi-supervised deep learning results," in *NeurIPS*, 2017.
- [39] J. Choi, T. Kim, and C. Kim, "Self-ensembling with gan-based data augmentation for domain adaptation in semantic segmentation," in *ICCV*, 2019.
- [40] J. Cha, H. Cho, K. Lee, S. Park, Y. Lee, and S. Park, "Domain generalization needs stochastic weight averaging for robustness on domain shifts," *arXiv preprint arXiv:2102.08604*, 2021.
- [41] Y. Chen, X. Zhu, and S. Gong, "Semi-supervised deep learning with memory," in *ECCV*, 2018.
- [42] K. He, X. Zhang, S. Ren, and J. Sun, "Deep residual learning for image recognition," in *CVPR*, 2016.
- [43] I. Goodfellow, J. Pouget-Abadie, M. Mirza, B. Xu, D. Warde-Farley, S. Ozair, A. Courville, and Y. Bengio, "Generative adversarial nets," in *NeurIPS*, 2014.
- [44] Y. Gal and Z. Ghahramani, "Dropout as a bayesian approximation: Representing model uncertainty in deep learning," in *ICML*, 2016.
- [45] P. Izmailov, D. Podoprikin, T. Garipov, D. Vetrov, and A. G. Wilson, "Averaging weights leads to wider optima and better generalization," in *UAI*, 2018.
- [46] L. Zhang, X. Li, A. Arnab, K. Yang, Y. Tong, and P. H. Torr, "Dual graph convolutional network for semantic segmentation," in *BMVC*, 2019.
- [47] L. Zhang, D. Xu, A. Arnab, and P. H. Torr, "Dynamic graph message passing network," in *CVPR*, 2020.
- [48] A. Paszke, S. Gross, S. Chintala, G. Chanan, E. Yang, Z. DeVito, Z. Lin, A. Desmaison, L. Antiga, and A. Lerer, "Automatic differentiation in pytorch," 2017.
- [49] G. Ros, L. Sellart, J. Materzynska, D. Vazquez, and A. M. Lopez, "The synthia dataset: A large collection of synthetic images for semantic segmentation of urban scenes," in *CVPR*, 2016.
- [50] W. Maddern, G. Pascoe, C. Linegar, and P. Newman, "1 Year, 1000km: The Oxford RobotCar Dataset," *The International Journal of Robotics Research (IJRR)*, vol. 36, no. 1, pp. 3–15, 2017. [Online]. Available: <http://dx.doi.org/10.1177/0278364916679498>
- [51] Y. Shan, C. M. Chew, and W. F. Lu, "Semantic-aware short path adversarial training for cross-domain semantic segmentation," *Neurocomputing*, vol. 380, pp. 125–132, 2020. [Online]. Available: <https://www.sciencedirect.com/science/article/pii/S0925231219315656>
- [52] M. Chen, H. Xue, and D. Cai, "Domain adaptation for semantic segmentation with maximum squares loss," in *Proceedings of the IEEE/CVF International Conference on Computer Vision*, 2019, pp. 2090–2099.
- [53] W. Zhou, Y. Wang, J. Chu, J. Yang, X. Bai, and Y. Xu, "Affinity space adaptation for semantic segmentation across domains," *IEEE Transactions on Image Processing*, vol. 30, pp. 2549–2561, 2020.
- [54] J. Yang, R. Xu, R. Li, X. Qi, X. Shen, G. Li, and L. Lin, "An adversarial perturbation oriented domain adaptation approach for semantic segmentation," in *AAAI*, 2020.
- [55] Z. Wang, M. Yu, Y. Wei, R. Feris, J. Xiong, W.-m. Hwu, T. S. Huang, and H. Shi, "Differential treatment for stuff and things: A simple unsupervised domain adaptation method for semantic segmentation," in *CVPR*, 2020.
- [56] T.-H. Vu, H. Jain, M. Bucher, M. Cord, and P. Pérez, "Advent: Adversarial entropy minimization for domain adaptation in semantic segmentation," in *CVPR*, 2019.
- [57] Y. Zhang, Z. Qiu, T. Yao, D. Liu, and T. Mei, "Fully convolutional adaptation networks for semantic segmentation," in *CVPR*, 2018.
- [58] G. Li, G. Kang, W. Liu, Y. Wei, and Y. Yang, "Content-consistent matching for domain adaptive semantic segmentation," in *ECCV*, 2020.
- [59] K. Simonyan and A. Zisserman, "Very deep convolutional networks for large-scale image recognition," *arXiv:1409.1556*, 2014.
- [60] Y. Zhang, P. David, and B. Gong, "Curriculum domain adaptation for semantic segmentation of urban scenes," in *ICCV*, 2017.
- [61] Q. Wang, J. Gao, and X. Li, "Weakly supervised adversarial domain adaptation for semantic segmentation in urban scenes," *IEEE Transactions on Image Processing*, vol. 28, no. 9, pp. 4376–4386, 2019.
- [62] I. Sutskever, J. Martens, G. Dahl, and G. Hinton, "On the importance of initialization and momentum in deep learning," in *International conference on machine learning*. PMLR, 2013, pp. 1139–1147.



Zhedong Zheng received the B.S. degree in computer science from Fudan University, China, in 2016. He is currently a Ph.D. student with the School of Computer Science at University of Technology Sydney, Australia. He was an intern at Nvidia Research (2018) and Baidu Research (2020). His research interests include robust learning for image retrieval, generative learning for data augmentation, and unsupervised domain adaptation.



Yi Yang received the Ph.D. degree in computer science from Zhejiang University, Hangzhou, China, in 2010. He is currently a professor with University of Technology Sydney, Australia. He was a Post-Doctoral Research with the School of Computer Science, Carnegie Mellon University, Pittsburgh, PA, USA. His current research interest includes machine learning and its applications to multimedia content analysis and computer vision, such as multimedia indexing and retrieval, video analysis and video semantics understanding.